Journal of Applied Mechanics and Technical Physics, Vol. 36, No. 1, 1995

DETERMINING THE STRAIN FEATURES OF ROCK JOINTS

L. A. Nazarov and E. N. Sher

UDC 539.3+622.83

It is generally recognized that a rock mass has a block structure [1] and that the contacts between blocks largely govern the behavior of the mass as a whole. Dynamic effects cannot be related solely to failure in the block material [1] and in the main there is rearrangement of the block system without block failure. An adequate description of strain in a rock mass and in the Earth's crust as a whole makes it extremely important to determine the characteristics of the block contacts.

The model for a block contact is an element of zero thickness whose force characteristics (tangential stress τ and normal stress σ) and strain characteristics (shearing R and approach P between the faces) are related by equations of state:

as proposed in [2]. One specifies the forms of T and S from laboratory experiments with specimens extracted from the mass, with the results then used to describe actual movements. A fairly detailed bibliography on this has been given in [3].

Basic contact features used in simulating the strain are the tangential rigidity K_t and the normal rigidity K_n, which are the coefficients of proportionality between the increments in the force and strain characteristics.

Various indirect methods such as [4, 5] are used when one cannot determine K_t and K_n by direct experiment, which are based on failure geometry and the properties of the constituent rocks.

The developed working system in a pit field provides in principle access to certain failure areas, while well-developed field measurement methods provide point values for the components of the stress tensor. The latter on the [6] basis can be interpolated to the failure points themselves. It appears favorable to organize a stationary acoustic-measurement point to determine not only the instantaneous strain characteristics but also the stress tendency around the area.

Here we propose a method of determining failure rigidities under real conditions, which is based on combining experiment with theory.

1. Determining Tangential Rigidity of a Contact Area when the Ends Are Accessible. A tester for examining block contacts [7] was used in an experiment whose scheme is shown in Fig. 1. Between the two lucite blocks B_1 and B_2 there were thin layers of various materials, and the entire system was subject to a horizontal stress F. Simultaneously, at each loading step, the contact was irradiated by the pulsed sound source S, whose signals were recorded by the sensors 1 and 2 (accelerometers). The length t_0 of the probe signal was chosen such that the wave reflected from the boundaries AB and CD did not distort the signal at the sensors for a time t_0.

Figure 2 shows the results (velocigrams for $\dot{w}$ as referred to the maximum value of $\dot{w}$ at the point of loading, with the solid lines for sensor 1 and the dashed lines for sensor 2) for various loading steps $\xi = F/F_0$ (F_0 the initial value). As the normal load increases, there is a reduction in the amplitude of the first onset A_1 at the sensor 1 closer to the source, while there is an increase in the amplitude A_2 and this in the ratio $\psi = A_2/A_1$, with reduction in φ $(t_2 - t_1)/t_0$ (t_i is the time of the maximum in the first arrival in the velocigram for sensor i, i = 1, 2).

The tangential rigidity of the contact was determined at each loading step in the x direction by rigid block displacement with measurement of the slope and the tangential stress, from which we calculated K_t. The dashed lines in Fig. 3 show ψ and φ in relation to the dimensionless rigidity $\bar{K}_t = K_t h/(\rho V_p^2)$ (ρ and V_p are the density of lucite and the speed of push waves in it, while h is the contact length, Fig. 1) as derived from the experimental data.

Novosibirsk. Translated from Prikladnaya Mekhanika i Tekhnicheskaya Fizika, No. 1, pp. 129-134, January-February, 1995. Original article submitted February 25, 1994.

0021-8944/95/3601-0123$12.50

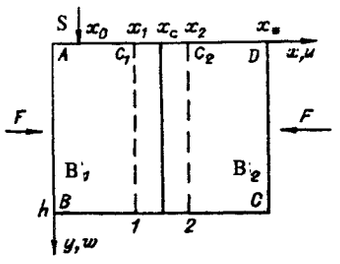

Fig. 1

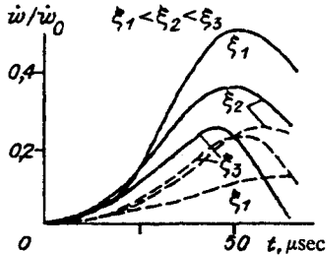

Fig. 2

The experiment scheme was examined theoretically on a planar model in an (x, y) cartesian coordinate system. The working region consisted of two elastic subregions having a common boundary (Fig. 1). The following conditions were set at the horizontal boundaries:

$$\sigma_y = \delta(x - x_0)f(t)H(t_0 - t),\ \tau_{xy} = 0 \quad \text{at} \quad y = 0; \tag{1.1}$$

$$\sigma_y = \tau_{xy} = 0 \quad \text{at} \quad y = h. \tag{1.2}$$

Here σ_x, σ_y, and τ_{xy} are components of the stress tensor, δ is a Dirac delta function, and H a Heaviside function; arbitrary homogeneous conditions apply at the vertical boundaries $x = 0$ and $x = x_*$, while the stresses are continuous on the contact line $x = x_c$ and the displacements are discontinuous:

$$\sigma_x = \bar{\sigma}_x = K_n P,\ P = u - \bar{u},\quad \tau_{xy} = \bar{\tau}_{xy} = K_t R,\ R = w - \bar{w} \tag{1.3}$$

(the quantities with overbars apply to the right-hand subregion). Boundary conditions (1.3) simulate the contact interaction for a linear dependence of the stresses on the relative displacements or the instantaneous situation if T and S are nonlinear.

Equations from the dynamic theory of elasticity apply in each subregion:

$$\begin{aligned}(\lambda + 2\mu)\frac{\partial^2 u}{\partial x^2} + \mu\frac{\partial^2 u}{\partial y^2} + (\lambda + \mu)\frac{\partial^2 w}{\partial x \partial y} &= \rho\frac{\partial^2 u}{\partial t^2},\\ (\lambda + 2\mu)\frac{\partial^2 w}{\partial y^2} + \mu\frac{\partial^2 w}{\partial x^2} + (\lambda + \mu)\frac{\partial^2 u}{\partial x \partial y} &= \rho\frac{\partial^2 w}{\partial t^2}.\end{aligned} \tag{1.4}$$

Here u and w are the displacements along x and y, while λ and μ are Lame parameters, ρ density, and t time.

System (1.1)-(1.4) was solved numerically by means of standard approximations providing the second order of accuracy. The only feature was linking up the solutions at $x = x_c$. There were no stresses at the horizontal boundaries near the joint, so it was possible to obtain uncoupled linear-equation systems for P and R, which were solved by the three-point method. The dimensional parameters were $\lambda + 2\mu$, ρ, and h, while the properties of the material in the subregions were identical. We chose x_0 and x_c such that the waves reflected from the side boundaries did not affect the signal at the points (x_i, h) corresponding to the sensors.

Calculations for the parameters corresponding to experiment ($x_0 = x_1 = 0.9$, $x_2 = 1.1$, $x_c = t_0 = 1$) confirmed the conclusions and showed that changes in K_t have very little effect on the behavior of $\dot{u}$, and the same for K_n as regards $\dot{w}$, so properly oriented sensors enable one to trace the behavior of the joint in different directions.

The solid lines in Fig. 3 show the theoretical $\psi(\bar{K}_t)$ and $\varphi(K_t)$, which fit experiment well. If the signal reception points lie directly at the edges of the contact ($x_1 = x_2 = x_c$), then $\psi \to 1$ and $\varphi \to 0$ for $K_t \to \infty$, i.e., the contact behaves as a continuous medium in one direction with increase in the corresponding rigidity.

The tangential rigidity may thus be determined as follows under field conditions. The theoretically calculated functions are $\psi(K_t)$, $\varphi(K_t)$, $\bar{K}_t = K_t/p$, $p = (\lambda + 2\mu)/m$, while m is the distance between source and detector (length of the joint section). The measurement point is arranged in accordance with Fig. 1 and one obtains the acoustic data (ψ_0 and φ_0, Fig. 3). Then the tangential rigidity of the working part is given by $K_t = p\psi^{-1}(\psi_0)$ or $K_t = p\varphi^{-1}(\varphi_0)$; the first is preferable because of the better resolution.

The experiments and calculations suggest

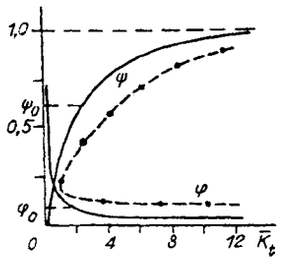

Fig. 3

$$K_t = K_t^* \frac{\sigma}{\sigma + \alpha}, \tag{1.5}$$

as relating the tangential rigidity and the normal stress at the contact. The two unknown parameters K_t^* and α are determined from two time-separated measurements on the static stresses $\sigma = \sigma_i$ and acoustic quantities $\psi = \psi_i$ (the latter gives K_t^i) after which one solves the system

$$K_t^i = K_t^* \frac{\sigma_i}{\sigma_i + \alpha}, \quad i = 1,2.$$

The second experiment may be replaced by a hypothesis (which in principle is confirmed qualitatively by these studies): for normal stresses close to the compressive strength $\sigma = \sigma_e$, the joint behaves as a continuous medium having $K_t = \mu/\varepsilon$ (ε is the visible contact thickness). One solves (1.5) for $\sigma \left(\sigma = \alpha \frac{K_t}{K_t - K_t^*}\right)$, to get a formula enabling one to make long-time observations on σ by the acoustic method.

Formula (1.5) gives a qualitatively good description of the [8] experiments. A formula proposed in [9] for the tangential rigidity is

$$K_t = A\sigma, \tag{1.6}$$

in which A is determined by direct shearing experiment. Instead, one can derive $A = K_t^0/\sigma_0$ by our method: acoustic measurements give $K_t = K_t^0$, and field measurements give $\sigma = \sigma_0$. Formula (1.6) follows from (1.5) or low stresses ($\alpha >> \sigma$).

2. Examining Rigidity Features of Joints with One-Sided Access. Access is not always available to the two ends of a joint (for example, when global faults emerge on the Earth's surface), so we consider a scheme for irradiating the contact with one-sided access. A vertical force is applied at the surface of the elastic region containing the joint displacement line (Fig. 1). At points on the surface on the two sides of the contact $C_i(x_i, 0)$ (i = 1, 2), one records the vertical accelerations $\ddot{w}$ and the horizontal ones $\ddot{u}$. One needs to derive the signal parameters corresponding to change in contact rigidity. The task is handled by means of a difference scheme similar to that in Section 1 but with the difference that $x_0 = 0$ and the lower boundary is eliminated. Calculations show that even at comparatively short distances from the joint (towards the source), the strain parameters do not influence the sensor readings, and that sensor can be used as the base one (i.e., the other data are normalized with respect to its readings).

Figure 4 shows

$$U(\bar{K}_t, \bar{K}_n) = \max|\ddot{u}(x_2,0,t)| / \ddot{w}_0, \; t_2 < t < t_0 + t_2,$$
$$W(\bar{K}_t, \bar{K}_n) = \max|\ddot{w}(x_2,0,t)| / \ddot{w}_0, \; t_2 < t < t_0 + t_2,$$

in which t_2 is the time of arrival of the perturbation at point C_2, and $\ddot{w}_0$ is the maximum vertical acceleration at the point $x_1 = 0.7x_c$; $x_2 = 1.3x_c$; $\bar{K}_t = K_t/q$; $\bar{K}_n = K_n/q$; $q = (\lambda + 2\mu)/x_c$.

TABLE 1

Points in Fig. 1	$\ddot{u}$	$\ddot{w}$
C_1	0,363	0,25
C_2	0,0225	0,033

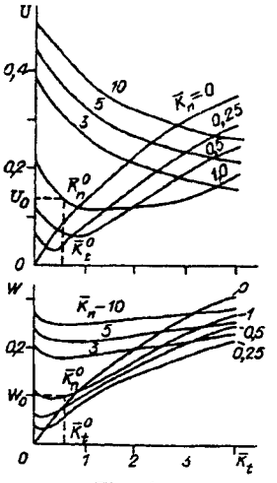

Fig. 4

Analysis shows that for any pair of values $U = U_0$ and $W = W_0$ one can quite accurately recover the corresponding values of $\bar{K}_t^0$ and $\bar{K}_n^0$, so it is in principle possible to estimate K_t and K_n under field conditions. Irradiation in the Fig. 1 schemes is required, and then the data from the sensors at point C_2 are normalized from the readings of the vertical sensor at point C_1, which gives U_0 and W_0. Then $U(\bar{K}_t, \bar{K}_n)$, $W(\bar{K}_t, \bar{K}_n)$ are calculated theoretically from these, and from U_0 and W_0 one derives the dimensionless rigidities $\bar{K}_t^0$, $\bar{K}_n^0$. The dimensional quantities are determined after the physical properties of the medium have been defined: $K_t^0 = q\bar{K}_t^0$, $K_n^0 = q\bar{K}_n^0$.

This approach was used to process the data from a model experiment on the properties of a joint layer with one-sided access.

The experiments were performed on a rectangular lucite plate $1 \times 1.5 \times 0.02$ m. There was a weakened layer along the median line of the large dimension formed by five rows of holes 10 mm in diameter with distances between centers of 12 mm, which simulated the block contact. The layer was irradiated by waves excited by impact on the face at the point x_0 (Fig. 1). At points C_1 and C_2 there were the detectors (accelerometer), which had $p = x_c - x_0 = 0.33$ m, $x_c - x_1 = x_2 - x_c = 0.1$ m. These recorded the vertical and horizontal accelerations of the free surface. The largest acceleration amplitudes occurred with Rayleigh waves, and they were recorded in the processing. The plate geometry allowed us to make the necessary recordings before the arrival of reflected signals from the other faces.

Table 1 gives the mean values of the relative maximum acceleration amplitudes found by recording a series of impacts. The relative accelerations at point C_2 gave $U_0 = 0.13$, $W_0 = 0.09$, and Fig. 4 gives the dimensionless rigidities $\bar{K}_t^0 = 0.6$, $\bar{K}_n^0 = 1$ in the weakened layer, where the dimensional values were as follows:

$$K_t^0 = 0{,}6(\lambda + 2\mu)/p,\ K_n^0 = (\lambda + 2\mu)/p.$$

Dynamic measurements gave $E = 5.4 \times 10^9$ Pa and $\nu = 0.32$ for lucite (Young's modulus and Poisson's ratio), whence $\lambda = 3.64 \times 10^9$ Pa and $\mu = 2.05 \times 10^9$ Pa. With these data and $p = 0.33$ m we have

$$K_t^0 = 14{,}1 \cdot 10^9 \text{ Pa/m},\quad K_n^0 = 23{,}4 \cdot 10^9 \text{ Pa/m}.$$

One can estimate the strain features of the weakened layer if one averages the elastic moduli over the medium containing holes. In our layer, the ratio of the area occupied by the solid medium to the total of the world medium with holes was $s = 0.45$. With layer thickness $b = 0.06$ m,

$$K_t = s\mu / b = 15{,}5 \cdot 10^9 \text{ Pa/m}, \quad K_n = sE / b = 41 \cdot 10^9 \text{ Pa/m}.$$

The calculated rigidities for the weakened layer were close to the experimental ones.

REFERENCES

1. M. A. Sadovskii, L. G. Bolkhovitinov, and V. F. Pisarenko, Strain in a Geophysical Medium and Seismic Processes [in Russian], Nauka, Moscow (1987).
2. R. E. Goodman, R. L. Taylor, and T. L. Brekke, "A model for the mechanics of jointed rock," Proc. ASCE, J. Soil Mech. and Found. Div., **94**, No. SM3, 637-659 (1968).
3. W. Wittke, Rock Mechanics, Springer-Verlag, Berlin (1990).
4. N. R. Barton and V. Choubey, "The shear strength of rock joints in theory and practice," Rock Mech., **10**, No. 1-2, 1-54 (1977).
5. Ke-Hsu-Sun, "Nonlinear analysis of a joint element and its application in rock engineering," Int. J. Numer. Analyt. Meth. Geomech., **5**, 220-245 (1981).
6. A. F. Revuzhenko and E. I. Shemyakin, "Some formulations of boundary-value problems in L plasticity," Prikl. Mekh. Tekh. Fiz., No. 2, 128-137 (1974).
7. A. V. Leont'ev and L. A. Nazarov, "Determining the rigidity of a contact between rock blocks," FTPRPI, No. 2, 46-52 (1994).
8. N. R. Barton, "Deformation phenomena in jointed rock," Geotechnique, **36**, No. 2, 147-167 (1986).
9. M. Oda, T. Wamabe, Y. Ishizuka, et al., "Elastic stress and strain in jointed rock masses by means of crack tensor analysis," Rock Mechanics and Rock Engineering, **26**, No. 2, 89-112 (1993).